

## Deeply Bound Hole States as a Giant-Resonance-Like Phenomenon\*

S. Y. van der Werf, B. R. Kooistra, W. H. A. Hesselink,† F. Iachello, L. W. Put, and R. H. Siemssen  
*Kernfysisch Versneller Instituut, Groningen, The Netherlands*

(Received 10 June 1974)

Giant-resonance-like peaks showing systematic variations with neutron number have been observed in the  $(d, t)$  reaction on the even- $A$  tin isotopes. In the reaction  $^{116}\text{Sn}(d, t)^{115}\text{Sn}$  a separation of the  $g_{9/2}$  and  $p_{1/2}, p_{3/2}$  neutron-hole components has been obtained. A calculation of the hole spectral function shows that shell effects play an important role in determining the spreading width.

Evidence for the excitation of deeply bound hole states in the  $(p, d)$  reaction was recently reported.<sup>1-3</sup> Over a broad range of excitation energies ( $E_x \approx 4-15$  MeV) the spectra from these pickup reactions are relatively featureless (except for a broad bump around 5 MeV excitation) and have the appearance of a continuous background. The angular distributions, however, obtained by integrating over the whole energy range are strongly forward peaked, and this suggests a predominantly direct reaction. It was therefore proposed<sup>1</sup> that the observed yield is due to pickup of neutrons from the next lower shell with the hole strength smeared out over very many levels.

As an alternative process we have studied the  $(d, t)$  reaction on tin at  $E_d = 50$  MeV. We observe at approximately 5 MeV excitation energy in the residual nucleus a very pronounced and giant-resonance-like structure which was also seen in the analogous  $(p, d)$  reaction<sup>1-4</sup> and, most recently, in the  $(^3\text{He}, \alpha)$  reaction.<sup>5</sup> From a measurement of the differential cross sections to extreme forward angles we were able to decompose the peak in the  $^{116}\text{Sn}(d, t)^{115}\text{Sn}$  spectrum into two distinct components with characteristic  $l=1$  and  $l=4$  angular distributions, respectively. Investigation of the  $(d, t)$  reaction on all even- $A$  isotopes of tin (with the exception of  $^{114}\text{Sn}$ ) allowed us to study the fragmentation (spreading width) of these deeply bound hole states as a function of neutron number.

Self-supporting targets of tin were bombarded with an energy-analyzed beam of 50-MeV deuterons from the Groningen azimuthally varying field cyclotron. Target thicknesses were 0.15, 1.53, 0.80, 2.10, 0.72, 0.30 mg/cm<sup>2</sup>, for the isotopes  $^{112,116,118,120,122,124}\text{Sn}$ , respectively. Spectra from the  $(d, t)$  reaction on these targets at  $\theta_{\text{lab}} = 15^\circ$  are shown in Fig. 1. These data were obtained with solid-state-detector telescopes with a typical resolution of  $\sim 150$  keV. For extreme forward angles from  $6-12^\circ$  a telescope with two

$\Delta E$  detectors and a stopping detector was used with two independent pulse multipliers for mass identification, giving  $(\Delta E_1 + \Delta E_2)E$  and  $\Delta E_1(\Delta E_2 + E)$ , respectively. Only those events were recorded that were accepted as tritons by both mass identifiers.

All the spectra reveal, at approximately the same  $Q$  value, a broad and giant-resonance-like peak riding on a continuous "background." The peak is narrowest and most structured for  $^{115,117}\text{Sn}$ . Quite remarkably it appears to broaden both toward smaller ( $^{111}\text{Sn}$ ) and larger neutron numbers though the  $^{112}\text{Sn}(d, t)^{111}\text{Sn}$  results are less certain because of possible contaminations. (In  $^{111}\text{Sn}$  a relatively narrow peak containing only one third of the integrated  $g_{9/2}$  cross section seen in  $^{115}\text{Sn}$  is riding on a broad gross-structure bump.) In addition to the gross-structure peaks there are indications of finer, intermediate-width structures superimposed onto the gross-structure peaks.

Close inspection of the gross-structure peak in the  $^{116}\text{Sn}(d, t)^{115}\text{Sn}$  reaction at the most forward angles (Fig. 2) reveals that it can be decomposed into a narrower ( $\sim 1.0$  MeV at the base) and a broader ( $\sim 2.5$  MeV wide) peak, as indicated at the top of Fig. 2, plus a "background." (Note that at  $6^\circ$   $l=1$  is strong and  $l=4$  is weak, and that at  $11.5^\circ$   $l=1$  has a minimum.) Angular distributions obtained for the broad and narrow peaks are shown in Fig. 3. These angular distributions have a very pronounced and diffractive pattern characteristic for a direct process for  $l=1$  and  $l=4$ , respectively. The curves in Fig. 3 are the results of distorted-wave Born-approximation calculations with the program DWUCK for pickup of a  $2p$  and a  $1g_{9/2}$  neutron employing the same optical-model parameters used to analyze<sup>6</sup> the reaction  $^{116}\text{Sn}(d, ^3\text{He})^{115}\text{In}$  at 50 MeV. Calculations with triton optical-model parameters for  $E_t = 20$  MeV<sup>7</sup> gave very similar results. The agreement between the data and the theoretical curves is striking. The hole strengths obtained from the

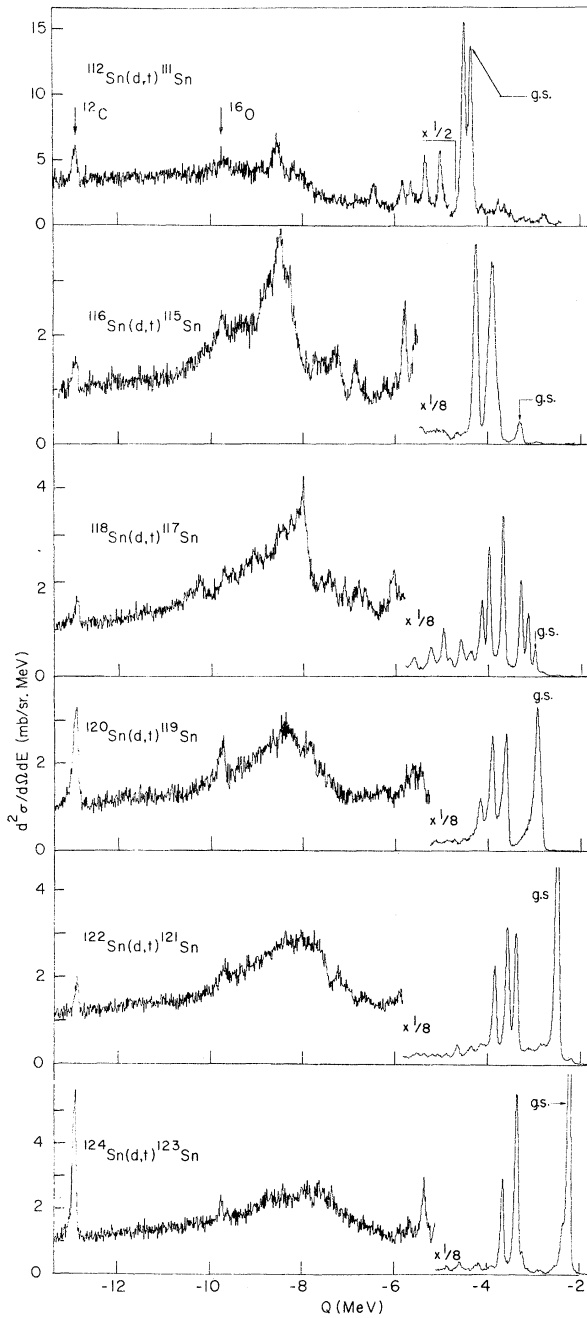


FIG. 1. Spectra from the reaction  $A\text{Sn}(d,t)^{A-1}\text{Sn}$  at  $15^\circ$  and  $E_d = 50$  MeV. Note the differences in scale for the low- and high-energy parts of the spectra.

distorted-wave Born-approximation analysis are  $\sim 30\%$  of the  $1g_{9/2}$  and  $\sim 20\%$  of the combined  $2p_{1/2}$ ,  $2p_{3/2}$  sum-rule limit for pickup of neutrons from the next lower shell.

The  $g_{9/2}$  and the  $p_{1/2}$ ,  $p_{3/2}$  holes are observed at 5–6 MeV excitation energy in the residual nuclei

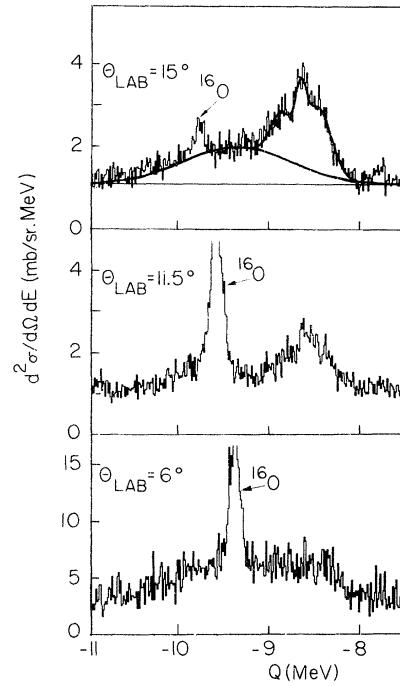


FIG. 2. Partial spectra showing the region around 5.5 MeV excitation in the reaction  $^{116}\text{Sn}(d,t)^{115}\text{Sn}$  indicating the separation of the gross structure into two components plus “background.”

in a region of very many ( $\sim 10^3/\text{MeV}$ ) levels. The bumps seen in the spectra thus represent a striking example of giant resonances in the sense of Lane, Thomas, and Wigner<sup>3</sup> in which the particle

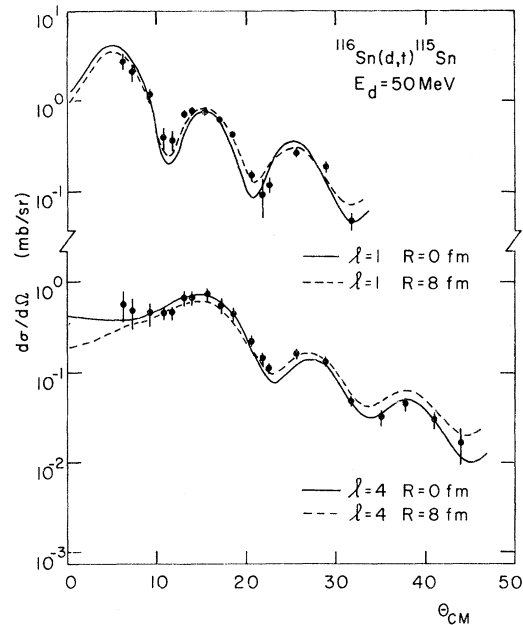


FIG. 3. Angular distributions of the two components of the gross structure shown in Fig. 2.

(hole) strength is distributed over very many, more complicated states. The arresting features of the present data are (i) the possibility to separate the  $l$  components according to different line shapes, (ii) the narrow width in  $^{115,117}\text{Sn}$ , and (iii) the apparent intermediate structure superimposed onto the gross structure of the bump. It is the relatively small spreading width of the observed hole states that makes them stand out over the "background" composed from pickup to the many underlying states with different spins and parities.

In order to understand the spreading mechanism we have performed a microscopic calculation similar in spirit to those of Bloch and Feshbach<sup>9</sup> and Shakin<sup>10</sup> of the spectral function

$$S_j(E) = \sum_{\sigma} |c_j^{\sigma}|^2 \delta(E - E^{\sigma}), \quad (1)$$

where the coefficients  $c_j^{\sigma}$  describe the admixture of the hole state  $j$  into eigenstates  $\sigma$  of the  $A-1$  nucleus at energies  $E^{\sigma}$ . By choosing to work in the BCS frame we automatically take into account pairing correlations in the ground state of the target nucleus. The calculation of the spectral function amounts to a diagonalization of the  $A-1$  Hamiltonian in the space spanned by the 1-qp, 3-qp, 5-qp, ... (quasiparticle) states. Proton excitations were not considered because of the  $Z=50$  closed shell.

Among the 3-qp, 5-qp, ... states the 1-qp +  $N$ -phonon ( $N=1, 2, \dots$ ) collective states have especially large matrix elements with the 1-qp states.<sup>11</sup> We have therefore separated the 3-qp, 5-qp, ... states into collective and noncollective states by introducing the operators  $Q$  and  $q$  projecting onto the collective and noncollective states, respectively. These, together with the projection operator  $P$  onto the 1-qp states, span the complete space. We have then treated the coupling between the  $P$  and  $Q$  space explicitly while considering that between the  $P$  and  $q$  space only on the average through a constant matrix element  $\langle v \rangle$ . The strength of the quadrupole and octupole interaction governing both  $P-Q$  and  $P-q$  couplings has been fixed by fitting the levels in the same  $A-1$  nucleus thus eliminating any adjustable parameter from the calculation. Since we are interested in excitation energies ( $\approx 5.5$  MeV) well below the threshold for particle emission ( $\approx 7.5$  MeV) the coupling to the continuum states has been neglected altogether.

According to the mechanism just described the single-hole state (1-qp) appears to be first fragmented into a discrete set of *collective* states

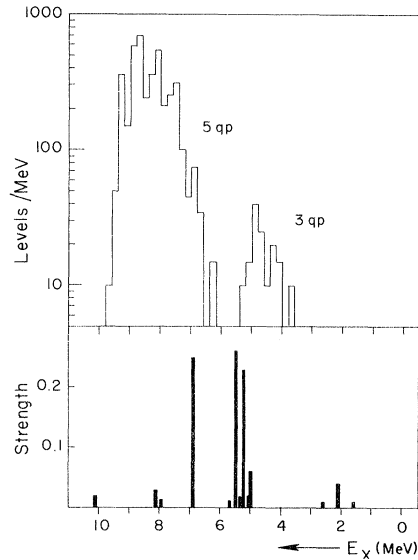


FIG. 4. Unperturbed level density of the  $\frac{9}{2}^+$  3- and 5-qp states in  $^{115}\text{Sn}$  obtained by direct counting of the number of states in  $\Delta E = 200$ -keV energy intervals (upper part). Fragmentation of the  $\frac{9}{2}^+$  hole strength due to the coupling with the 1-qp + phonon collective states (lower part).

(1-qp + phonons) and subsequently spread over the many underlying noncollective states (3-qp and 5-qp). The fragmentation gives rise to the intermediate structure. Since the spreading width is, in first approximation, given by

$$\Gamma = 2\pi\rho |\langle v \rangle|^2, \quad (2)$$

where  $\rho$  is the density of the 3- and 5-qp noncollective states, variations in the gross structure, as those experimentally observed, are to be attributed to differences in the local level density of the 3- and 5-qp noncollective states. Indeed our calculation shows that at 5–6 MeV this level density is still subject to *shell effects*, and therefore large differences in the spreading widths from one nucleus to the other are to be expected. In particular the narrow width observed in  $^{115,117}\text{Sn}$  seems to be connected with the partial shell closure at  $N=64$  which gives rise to a "gap" in the level density as shown for  $^{115}\text{Sn}$  in Fig. 4. The smaller density at the energy where most of the fragmented  $g_{9/2}$  strength lies (shown in the lower part of Fig. 4.) lets it clearly stand out over the "background." In contrast no such effect appears to be present in the other Sn isotopes and this would explain the larger spreading width found for these nuclei.

The assistance of B. Fryszczyn during some

phases of the data taking is gratefully acknowledged.

\*Work supported in part by the Stichting Voor Fundamenteel Onderzoek der Materie.

†Present address: Vrije Universiteit, Amsterdam, The Netherlands.

<sup>1</sup>M. Sakai and K. Kubo, Nucl. Phys. **A185**, 217 (1972).

<sup>2</sup>T. Ishimatsu, S. Hayashibe, N. Kawamura, T. Awaya, H. Ohmura, Y. Nakajima, and S. Mitara, Nucl. Phys. **A185**, 273 (1972).

<sup>3</sup>T. Ishimatsu, S. Hayashibe, T. Awaya, and H. Ohmura, J. Phys. Soc. Jpn. **35**, 1579 (1973).

<sup>4</sup>F. E. Bertrand and R. W. Peelle, Phys. Rev. C **8**, 1045 (1973), and private communication.

<sup>5</sup>M. Sakai, M. Sekiguchi, F. Soga, Y. Hirao, K. Yagi, and Y. Aoki, Phys. Lett. **51B**, 51 (1974).

<sup>6</sup>W. H. A. Hesselink, B. R. Kooistra, L. W. Put, R. H. Siemssen, and S. Y. van der Werf, Nucl. Phys. **A226**, 229 (1974).

<sup>7</sup>E. R. Flynn, D. D. Armstrong, J. G. Beery, and A. G. Blair, Phys. Rev. **182**, 1113 (1969).

<sup>8</sup>A. M. Lane, R. G. Thomas, and E. P. Wigner, Phys. Rev. **98**, 693 (1955).

<sup>9</sup>B. Bloch and H. Feshbach, Ann. Phys. (New York) **23**, 47 (1963).

<sup>10</sup>C. Shakin, Ann. Phys. (New York) **22**, 373 (1963).

## Resolving Ambiguities in Heavy-Ion Potentials\*

D. A. Goldberg and S. M. Smith†

University of Maryland, College Park, Maryland 20742

(Received 16 April 1974)

It is shown that nuclear (as opposed to Coulomb) rainbow-scattering data would be useful in discriminating among heavy-ion optical potentials. Acquisition of such data is facilitated by going to higher bombarding energies and using low-*A* targets.

There has recently been a great deal of interest in obtaining optical potentials which will satisfactorily describe the elastic scattering of heavy ions and which can be used in distorted-wave Born-approximation calculations for transfer reactions.<sup>1</sup> Most of the experiments performed to date appear to be sensitive only to the extreme tail of the nuclear potential, and hence, if one assumes that the potential is of the Woods-Saxon form,

$$U(r) = \frac{-(V + iW)}{1 + \exp[(r - R)/a]},$$

one can only determine *a* and the combined constant  $(V + iW)e^{R/a}$ . The situation is very similar to that which existed for the early  $\alpha$ -scattering experiments.<sup>2</sup> It therefore appears reasonable that recent approaches which have proven helpful in unraveling the ambiguities in  $\alpha$ -particle scattering may also prove useful for heavy ions and possibly prevent some retracing of familiar, if not altogether fruitful, ground as well.<sup>3</sup>

In a recent paper by the present authors<sup>4</sup> it was shown that discrete ambiguities in the  $\alpha$ -particle optical potential could be resolved<sup>5</sup> by taking data beyond the maximum *negative* deflection angle or *nuclear* rainbow angle  $\Theta_r^{(N)}$ .<sup>6</sup> This result can be explained in classical terms. Since the maximum deflection angle increases with the

strength of the potential, measurement of the former quantity determines the latter. In both the classical and quantum cases, the measurement is effected by measuring the cross section in the region beyond the maximum deflection angle  $\Theta_r^{(N)}$ . In the classical case, the cross section falls abruptly to zero beyond  $\Theta_r^{(N)}$ ; in the quantum case, it exhibits the exponential-like fall-off characteristic of rainbow scattering.

One might well expect that nuclear-rainbow-scattering data would be useful in eliminating ambiguities other than the discrete kind. In particular, for  $Ve^{R/a}$  ambiguities, the parameter *a* is well determined, and so the maximum deflecting force, which occurs at  $r = R$ , is simply proportional to *V*. It is our purpose to show, by using a series of model calculations, that the above expectation appears to be justified, and to examine the experimental conditions which would facilitate the observation of nuclear rainbow scattering.

It was shown in Ref. 4 that there is a minimum energy  $\epsilon_{\text{crit}}$  required for nuclear rainbow scattering to occur, and that as the energy is increased above  $\epsilon_{\text{crit}}$ , the nuclear rainbow angle  $\Theta_r^{(N)}$  decreases to smaller (and experimentally more accessible) angles. To verify this for the case of heavy ions, we have performed model calculations for the case of <sup>16</sup>O incident on <sup>28</sup>Si.